
Divide-and-Shuffle Synchronization for Distributed Machine Learning

Weiyan Wang ^{*}, Cengguang Zhang ^{*}, Liu Yang ^{*}, Jiacheng Xia ^{*}, Kai Chen ^{*}, and Kun Tan ⁺

^{*} Hong Kong University of Science and Technology

{weiyan.wang, czhangch, lyangau, jxiaab}@connect.ust.hk, kaichen@cse.ust.hk

⁺ Huawei

kun.tan@huawei.com

Abstract

Distributed Machine Learning suffers from the bottleneck of synchronization to all-reduce workers' updates. Previous works mainly consider better network topology, gradient compression, or stale updates to speed up communication and relieve the bottleneck. However, all these works ignore the importance of reducing the scale of synchronized elements and inevitable serial executed operators. To address the problem, our work proposes the Divide-and-Shuffle Synchronization(DS-Sync), which divides workers into several parallel groups and shuffles group members. DS-Sync only synchronizes the workers in the same group so that the scale of a group is much smaller. The shuffle of workers maintains the algorithm's convergence speed, which is interpreted in theory. Comprehensive experiments also show the significant improvements in the latest and popular models like Bert, WideResnet, and DeepFM on challenging datasets.

1 Introduction

Distributed Machine Learning is an efficient solution to train complex deep models on large volumes of data. The success of modern machine learning usually depends on both factors. Public large data sets like ImageNet [1] and BooksCorpus [2] are not only benchmark but also prior knowledge for fine-tuning. On-line services like recommendation systems have benefited a lot in making use of the accumulated user logs. Complex deep models usually can achieve state-of-the-art performance on such big data, but models like Wide-Resnet [3], Bert [4] and DeepFM [5] may take days to train. Distributed machine learning can make a difference by making use of more data or model parallelism.

Nowadays, popular deep learning frameworks such as Pytorch, Tensorflow, and Mxnet inherently support data-parallel distributed training. However, distributed machine learning suffers from the significant bottleneck of synchronization of all workers. Despite that all workers' compute gradients in parallel, different workers need to synchronize and average all gradients to update model parameters uniformly. This all-reduce synchronization operation among workers means slow network communication, serial execution, and idle waiting time, which takes considerable time during training. Previous works mainly consider how to make synchronization operation faster by better topology [6, 7] for full bandwidth, gradient compression [8, 9] and local SGD [10] for less data transferring, or stale update [11] to avoid waiting. But those previous works have not made any attempts to decrease the scale of synchronization for less inevitable serial executed operators, ignoring that it is highly related to the synchronization cost.

To this end, we propose Divide-and-Shuffle Synchronization(DS-Sync) to address the problem above. Dividing workers into groups and shuffling workers across groups are the two key factors of DS-Sync. In Figure 1, we compare the DS-Sync with the Bulk Synchronization Parallel(BSP) in a

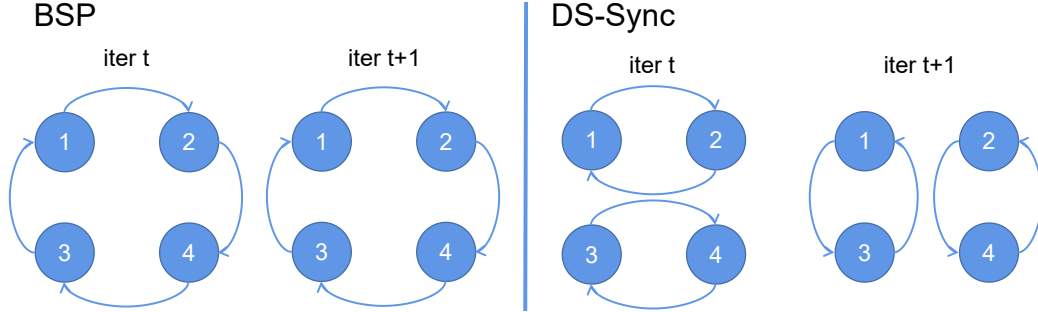


Figure 1: BSP synchronizes all workers in every iteration. Its scale of synchronization is 4, and it needs $4 + 4 - 1 = 7$ communications to average and broadcast one parameter in the ring all-reduce. DS-Sync divides four workers into two parallel groups of two workers, and the synchronization scale is halved to 2 within each group. Groups can synchronize simultaneously, and it needs 2 groups of 2 communications(28.6% of BSP) in parallel and 4 times(57.1% of BSP) in total. The two groups exchange workers every iteration so worker 1 can get information about 3,4 in the iteration $t + 1$.

simple scenario of 4 workers. In the t -th iteration, all workers are divided into multiple groups, and only workers in the same group will synchronize and communicate. Then the scale of an all-reduce synchronization operation is reduced at least by half(in only two groups case), and different groups can synchronize in parallel without conflicts. Then in the next iteration $t + 1$, the workers will be shuffled and exchanged among groups in a designed pattern. By shuffling and exchanging within groups, a worker can synchronize and communicate with unseen workers in the last iteration. Intuitively, shuffling makes every worker get the global update information from all workers in certain iterations instead of every iteration. Furthermore, Divide-and-Shuffle operations may have some positive side effects on generalization. The divide operation reduces the practical batch size, and shuffle operation adds stochastic noises, which both have the potential to make the training model easier to jump out of sharp minima to reach flatter one. In Section 3.3, we conduct a detailed analysis to explain the convergence performance of DS-Sync in the convex and non-convex cases respectively. To verify its effectiveness, we conduct comprehensive experiments by using the modern challenging data sets, including SQuADv1.1, ImageNet, Cifar10/100, and Criteo. We also challenge the latest and popular deep models, including Wide-Resnet, Bert and DeepFM and state-of-the-art optimizers, including Adam, AdamW, and SGD with momentum.

Overall, we propose the novel DS-Sync for distributed learning to speed up the wall time of converging on modern deep models and large data sets. Our contributions can be summarized in 3 aspects:

1. We explore a new direction in reducing the scale of synchronization for less serial executed operations. It relieves the bottleneck and decreases the iteration overhead, resulting in improved system throughput.
2. We maintain the same converged accuracy and speed as BSP. Divide-and-Shuffle operations have even added positive side-effects to help converge and generalize better.
3. We make a theory analysis on DS-Sync about its scale of synchronization and convergence.

2 Related Work

Distributed machine learning has been an active area even before deep learning emerged. Earlier works tend to design job-specific approaches to do model updates [12, 13, 14, 11] other than a unified framework. More recently, Parameter Server(PS) [15] gives a general sub-gradient descent framework suitable for a wide range of models. Although existing frameworks provide decent scalability by parallel gradient computing among workers, they still suffer from the bottleneck of synchronizing all workers. The previous works in speeding up synchronization can be categorized as followings:

- Improving Bandwidth Utilization: Traditional PS has the many-to-one communication problem when parameter servers are less than workers, resulting in a single-node network bottleneck. Ring All-Reduce makes use of the ring-like topology to realize all one-to-one communication for full bandwidth utilization [6]. Similarly, Tree All-reduce also slices

data into different sets and set up multiple hierarchical trees with different weights to make in-degree and out-degree of all nodes balanced for full usage of bandwidth. The works in this category focus on making full use of all links and bandwidth to transfer a large array of data.

- Reducing Data Transferring: There are extremely rich works studying precision-speed tradeoff to decrease transferred data size. Gradient compression [8, 16] only transmits the gradients that matter, such as gradients in large magnitudes. Quantization [9] uses lower precision variables to represent gradients and parameters to reduce network load. Local SGD [10] decreases the frequency of global synchronization by holding the gradients and taking several local updates before one global update.
- Relaxing the synchronization: Another line of research relaxes the synchronization requirements to achieve higher throughput. Instead of synchronization at every batch [17], Stale synchronous parallel [11] allows some workers, especially the stragglers, to skip synchronization. Some other methods [18] propose fully asynchronous parallel(ASP) computations among all workers. However, recent studies [19] show these methods seem to work only for limited models and vallina SGD optimizer. They are prone to poor convergence speed and quality in advanced optimizers with momentum like Adam and modern deep models.

However, our work DS-Sync explores a new direction in reducing the synchronization scale for less inevitably serial executed operations and lower probability of idle waiting. It is orthogonal with the works about bandwidth utilization improvement and transferred data reduction. In DS-Sync, it can use those techniques in the group synchronization to further improve overall performance. Unlike previous works relaxing the synchronization constrains, DS-Sync does not sacrifice the convergence, and it can work on modern deep models and advanced optimizers such as Adam, AdamW, and SGD with momentum. It is also noteworthy that our work is not a directly divide-and-conquer synchronization in a hierarchical structure. DS-Sync divides workers into multiple parallel groups and depends on shuffling workers to get global information.

3 Methodology

In this section, we discuss the methodology of DS-Sync. Firstly, we make an introduction to the details of the DS-sync method. Then we analyze the communication and synchronization complexity of DS-Sync. Finally, we make a theory convergence analysis in both convex and non-convex cases.

3.1 DS-Sync Algorithm

Algorithm 1 Optimization with Divide-and-Shuffle Synchronization

```

Require: Rank, WorldSize, GroupSize
Ensure: WorldSize == GroupSize*GroupSize
1: ## all workers initialize in the same way
2:  $model_{rank} = model_0$ 
3: for  $t = 0$  to TotalIteration do
4:   ## sample a local batch
5:    $input, target = DistributedDataLoader(Rank)$ 
6:    $output = model_{Rank}(input)$ 
7:    $loss = LossCriteron(output, target)$ 
8:    $gradient = loss.backward()$ 
9:   ## local model parameters updated on local batch
10:   $model_{Rank}.optimizer\_step(gradient)$ 
11:  if  $t \% 2 == 0$  then
12:    ## 4 nodes:[0,1][2,3], 9 nodes: [0,1,2][3,4,5][6,7,8]...
13:     $group = \{x | x \% GroupSize == Rank \% GroupSize \text{ and } x \leq WorldSize\}$ 
14:  else
15:    ## 4 nodes:[0,2][1,3], 9 nodes: [0,3,6][1,4,7][2,5,8]...
16:     $group = \{x | x \% GroupSize == Rank \text{ and } x \leq WorldSize\}$ 
17:  end if
18:  ## average the model parameters within the same group
19:   $AverageAllReduce(model_{Rank}, group)$ 
20: end for

```

We show the overview of the DS-Sync in Algorithm 1 and assume that world size(total worker number) is the square of group size for convenience. As the same as the previous distributed machine

learning methods, we randomly and evenly split the training data set across the workers. Every worker randomly samples a batch from its own set every iteration and compute local gradients of local batch as shown in lines 2-6. But different from standard BSP that all-reduces the local gradients, DS-Sync algorithm use local gradients to update local model(in the line 8) and all-reduces the parameters instead(in the line 17). Formally, we can define the weight update rules as the Equation 1:

$$w_{t+1}^i = \frac{1}{N} \sum_{j \in \text{Group}^{(i)}} \hat{w}_{t+1}^j \quad \text{where} \quad \hat{w}_{t+1}^j = w_t^j - \alpha \Delta_{t+1}^j \quad (1)$$

where w_t^i is the synchronized weight on i -th worker in the iteration t , \hat{w}_t^i is the local updated weight by local gradients on i -th worker in the iteration t , N is the group size, $j \in \text{Group}^{(i)}$ stands for all workers in the group containing i -th worker, α is the learning rate, and Δ_{t+1}^j is the $t+1$ time-step update of optimizer in j -th worker. We also do the same average all-reduce on the non-learnable model statistical parameters such as moving average and moving variance in batch norm layers. But we do not synchronize the statistical states of the optimizer such as moving averages (momentum) and moving square mean of gradients.

The division patterns of groups alter between consecutive N worker ranks(in lines 12 and 13: $\{x|\text{if } x//\text{GroupSize} = \text{Rank}\}$) and worker ranks jumping every N steps(in lines 15 and 16: $\{x|\text{if } x\% \text{GroupSize} = \text{Rank}\}$) in the period of two. Therefore, any group in iteration $t+1$ is consist of workers from all groups in last iteration t . Groups in iteration $t+1$ are the same as ones in iteration $t-1$, which means workers in the same group of iteration $t+1$ should share the same weight w_{t-1} in the iteration $t-1$. Obviously, any worker i can get update information from all workers every 2 iteration. Formally, it can be derived as follows:

$$\begin{aligned} w_{t+1}^i &= \frac{1}{N} \sum_{j \in \text{Group}^{(i)}} \hat{w}_{t+1}^j = \frac{1}{N} \sum_{j \in \text{Group}^{(i)}} (w_t^j - \alpha \Delta_{t+1}^j) \\ &= \frac{1}{N^2} \sum_{j \in \text{Group}^{(i)}} \sum_{k \in \text{Group}^{(j)}} (w_{t-1}^k - \alpha \Delta_t^k) + \frac{1}{N} \sum_{j \in \text{Group}^{(i)}} -\alpha \Delta_{t+1}^j \\ &= \frac{1}{W} \sum_{k=0}^W (w_{t-1}^k - \alpha \Delta_t^k) + \frac{1}{N} \sum_{j \in \text{Group}^{(i)}} -\alpha \Delta_{t+1}^j \end{aligned} \quad (2)$$

Where $W = N^2$ stands for the world size. Clearly, the Equation 2 says that any worker i in iteration $t-1$ can see the t -th updates and $(t-1)$ -th weights of all workers.

3.2 Synchronization Scale Analysis

The cost of all-reduce synchronization should be $\frac{SD}{B}$, where S is the scale of synchronization, D is the total data size, and B is the bandwidth for transferring one element. Previous works in all-reduce synchronization only focus on the better topology to improve bandwidth B for a large array of data. PS offers multiple P parameter servers for different slices of data to relieve many-to-one bottleneck. Ring All-reduce transfers parameters in a circle so that there is only one-to-one transferring. Tree All-reduce slices data into different sets and set up N trees with different weights to make in-degree and out-degree of all nodes balanced to make full use of bandwidth B . However, all these works ignore the possibility of reducing S the scale of synchronizing one element.

Here we formally define the Synchronization Scale in distributed machine learning in the Definition 3.1 as following:

Definition 3.1. Distributed Machine Learning Synchronization Scale: It is the number of inevitable serial executed and costly operations in synchronizing one element, typically one parameter of the model, among the needed workers.

For the PS, the pull operation needs W communications from W workers, and so does the push operation. Namely, the synchronization scale of PS is $2W$. For the Ring All-Reduce, one parameter takes W steps to traverse the ring for the reduction and need to take another $W-1$ steps to broadcast. For the Binary Tree All-Reduce, the reduction is from leaves to the root, while the broadcast is from the root to leaves. If and only if nodes in the same layer do not have the same parent, the reduction

Table 1: The Synchronization Scale and Overall Cost Comparision

	Bandwidth	Scale of Sync	Overall Cost
PS	BP/W	$2W$	$2W^2D/PB$
Ring All-reduce	B	$2W - 1$	$(2W - 1)D/B$
Tree All-reduce	B	$3 \log W$	$3 \log WD/B$
DS-Sync(Ring within the group)	B	$2\sqrt{W} - 1$	$(2\sqrt{W} - 1)D/B$
DS-Sync(Tree within the group)	B	$3 \log \sqrt{W}$	$3 \log \sqrt{WD}/B$

is in parallel and estimated to be $2\log W$. The broadcast in the same layer is always in parallel and should be $\log W$.

However, our proposed solution DS-Sync divides all W workers into $N = \sqrt{W}$ groups and synchronization scale is reduced to be $N = \sqrt{W}$. All-reduce synchronization operations in different groups are in parallel. Additionally, DS-Sync is independent of the topology. Within a group, all previous works like Ring and Tree All-reduce can be used to make full use of bandwidth. Therefore, we make a clear comparison in the Table 1 . DS-Sync can at least halve the synchronization scale and overall cost even in the case of Tree All-reduce or W is as small as 4. It can even achieve larger advantages like only one quarter when the W is 16 and using Ring All-reduce or PS as the topology.

3.3 Understanding Convergence of the DS-Sync

We start with the a simplified case to see why DS-Sync works, in which $L(X)$ is both convex and smooth and vanilla SGD is the local optimizer in line 10 of the Algorithm 1. Specifically, We make assumptions as follows:

Assumption 3.1. $L(X)$ is strict convex problem with $F(\frac{x_1+x_2}{2}) \leq \frac{F(x_1)+F(x_2)}{2}$. Both $L(X)$ and its gradient function $\nabla L(X)$ are L-Lipschitz smooth, namely $|\nabla F(x_1) - \nabla F(x_2)| \leq L|(x_1 - x_2)|$ and $|\nabla F(x_1) - \nabla F(x_2)| \leq H|(x_1 - x_2)|$. The learning rate every step is bounded and small enough.

Informally, we can show the DS-Sync converge in this case as followings: In the local updating, it is obvious that the local updated weights \hat{w}_t^i is expected to have lower loss and be closer to optimal weight w^* than w_{t-1}^i . In other words, we have $E(L(\hat{w}_t^i)) \leq E(L(w_t^i))$ and $E(D(\hat{x}_t^i|x^*)) < E(D(x_t^i|x^*))$ where $D(x_1|x_2) = (x_1 - x_2)^2$. The proof for the local updating part is just the same as the classical SGD algorithm. In the coming group synchronization synchronization, the whole group workers' weights are set to $\frac{1}{N} \sum_{j \in \text{Group}} \hat{w}_{t+1}^j$. Considering the definition of strict convex function, we can have the conclusion that $L(w_{t+1}) = L(\frac{1}{N} \sum_{j \in \text{Group}} \hat{w}_{t+1}^j) \leq \frac{1}{N} \sum_{j \in \text{Group}} L(\hat{w}_{t+1}^j)$. It means that $L(w_{t+1})$ is at least less than the $\text{argmax}_L(\hat{w}_t^i)$. What is more, $L(w_{t+1})$ may be less than any $L(\hat{w}_t^i)$ and speed up the convergence, if there are \hat{w}_t on the opposite sides of x^* . Therefore, we can find a virtual tool sequence X that $x_{2i} = w_i$ and $x_{2i+1} = \text{argmax}_L(\hat{w}_t^i)$, and it always holds for $E(L(x_{i+1})) \leq E(L(x_i))$.

When coming to modern complex deep models, it is impossible to hold the Assumption 3.1 everywhere. The deep models are non-convex with many minimums like sharp and flat ones, resulting in no guarantee of reaching the global minimum. But the convex and smooth conditions may hold in a small local area such as the neighborhood of a flat minimum where the loss change is slow. Compared with sharp minimums, some works [20] argue that flat minimums are preferred for better generalization. DS-Sync can work when all workers enter the neighboring area of the same flat minima. When some workers get stuck in sharp minima, the DS-Sync may get better chances to jump out for the following two reasons:

1. Decreased Batch Size in Practice: DS-Sync divides workers into multiple groups to synchronize, making that new w_{i+1} only depends on one group of workers instead of all workers as shown in Equation 1. The smaller batch size in practice brings in more variances during optimization, making it less stable to stay in a sharp and narrow minimum.
2. Stochastics from Shuffling: DS-Sync also shuffles the group members in every iteration, resulting in that $w_i^{j \in \text{group}}$ weights do not share the same initial value before local updating. Although all $w_i^{j \in \text{group}}$ are supposed to be close, it makes the gradients noisier to jump out, if the loss change is not so smooth as in a flat minimum.

4 Experiments

The experiment results of DS-Sync are shown in this section. We start by discussing the detailed experiment settings. We show that DS-Sync maintains at least the same convergence speed if it is not better than BSP. Furthermore, we find a considerable reduction in iteration overhead because of the decreased scale of synchronization. Finally, we verify that DS-Sync leads to a significant improvement in the wall time of convergence for the target accuracy.

4.1 Experiment Settings

We use CIFAR10/100 [21], ImageNet [1], SQuADv1.1 [22] and Criteo¹ four famous data sets widely used in Computer Vision, Natural Language Processing, and Recommendation System. We follow the standard pre-process and data split. Specifically, CIFAR10/100 has 50000 training images and 10000 test images. ImageNet has 1.28 million training images and 50k validation images to evaluate. SQuAD v1.1 is a collection of over 100,000 question-answer pairs on over 500 articles. Criteo data set includes 45840617 users' click records. For both SQuAD v1.1 and Criteo data sets, we split it into two parts: 90% is for training, while the rest 10% is for testing.

We use PyTorch to develop our DS-Sync and all baselines, including BSP and ASP. NCCL library is the default communication method for DS-Sync and BSP, while ASP has to use the send and receive functions in Gloo to realize the pull-push operation. We train CIFAR10/100 on WRN-26-10 and ImageNet with WRN-50-2 by SGD momentum and share the same hyperparameters of initial learning rate(LR): 0.1, momentum: 0.9, and weight decay: 0.0001 for convenience. In Cifar10/100, LR decrease by 0.2 in epochs 60, 120, 160. Cifar10 sets 256 as the batch size per GPU, while Cifar100 uses 128. But in ImageNet, LR decrease by 0.1 in epochs 30 and 60, and batch size per GPU is 30. We fine-tuned the SQuADv1.1 dataset on the pre-trained BERT-Large model(bert-large-uncased-whole-word-masking). We set the batch size per GPU as 6 to fulfill GPU memory. AdamW optimizer is used with LR: 3e-5, epsilon equals: 1e-8, weight decay: 0, and betas: 0.9 and 0.999. We trained a DeepFM model on Criteo data with Adam. We set batch size per GPU as 20480. Other hyperparameters includes LR: 1e-3, weight decay: 1e-5 and betas: 0.9 and 0.999. Unless specified, all experiments are repeated by five times for 4-node experiments and three times for 16-node experiments except that ImageNet only runs for once.

We use a private cluster of 16 nodes as our environment for stable speed measurement. Each node has one NVIDIA V100 Tensor Core GPU, Intel Xeon E5-2686 v4, 2.7 GHz, a memory of 61GiB. 10GB Ethernet fully connects all the nodes. The configuration is quite representative in the data center since it is similar to commercial AWS P3.2xlarge instances. We have open-sourced our code and make it available on Github website: <https://github.com/OutstanderWang/Divide-and-Shuffle>.

4.2 Convergence Results

We firstly verify and compare the convergence performance of DS-Sync in terms of best test accuracy and iteration numbers. The Table 2 shows the best test accuracy of DS-Sync and baselines in the small-scale case of 4 nodes. We find that DS-Sync has at least the same accuracy as the BSP, while ASP is considerably lower. In the large-scale scenario of 16 nodes as shown in Table 3, the test accuracy

Table 2: Converged Accuracy Comparison in 4 nodes

		Accuracy	LogLoss			Exact Match	F1
Cifar10	BSP	90.00% $(\pm 1.69\%)$	0.4655 (± 0.0881)	SQuAD	BSP	93.06% $(\pm 0.22\%)$	86.85% $(\pm 0.53\%)$
	ASP	87.46% $(\pm 1.31\%)$	0.5348 (± 0.0676)		ASP	89.94% $(\pm 0.36\%)$	82.72% (± 0.46)
	DS-Sync	91.63% $(\pm 0.76\%)$	0.4082 (± 0.0424)		DS-Sync	93.01% $(\pm 0.26\%)$	86.83% $(\pm 0.56\%)$
Cifar100	BSP	75.86% $(\pm 0.28\%)$	1.1406 (± 0.0148)	Criteo	BSP	AUC	LogLoss
	ASP	66.23% $(\pm 0.23\%)$	1.5557 (± 0.0963)		ASP	80.51% $(\pm 0.03\%)$	0.4469 (± 0.0005)
	DS-Sync	75.78% $(\pm 0.39\%)$	1.1357 (± 0.0200)		DS-Sync	80.48% $(\pm 0.07\%)$	0.4494 (± 0.0036)
ImageNet	BSP	top1:73.10% top5:91.34%	1.1743			80.50% $(\pm 0.02\%)$	0.4469 (± 0.0004)
	DS-Sync	top1:73.25% top5:91.35%	1.1574				

of all methods decreased resulted from larger overall batch size. But we observe that DS-Sync is less influenced by it and has marginal advantages over BSP. It is because 16 nodes means 4 groups and more stochastics than the 4-node case. We have interpreted the reasons for it in Section 3.3

¹<http://labs.criteo.com/downloads/2014-kaggle-display-advertising-challenge-dataset/>

Table 3: Converged Accuracy Comparision in 16 nodes

		Accuracy	LogLoss		Exact Match	F1
Cifar10	BSP	85.14%($\pm 3.11\%$)	0.5894($\pm 0.1457\%$)	SQuAD	BSP	92.66%($\pm 0.08\%$)
	DS-Sync	88.46%($\pm 1.56\%$)	0.4402($\pm 0.0433\%$)		DS-Sync	92.64%($\pm 0.01\%$)
Cifar100	BSP	72.60%($\pm 0.43\%$)	1.4630($\pm 0.0047\%$)	Criteo	BSP	80.47%($\pm 0.08\%$)
	DS-Sync	73.09%($\pm 0.20\%$)	1.4441($\pm 0.0060\%$)		DS-Sync	80.48%($\pm 0.08\%$)
					AUC	0.4465($\pm 0.0007\%$)
					LogLoss	
						0.4464($\pm 0.0007\%$)

The converge curve in Figure 2 also shows that DS-Sync has faster or comparable converge speed for all models and cases compared to BSP, while ASP's curve is lower. We exclude the ASP as the baseline in 16 nodes and for ImageNet in 4 nodes because it is not inclined to converge properly. We also omit all ImageNet experiments in 16 nodes because of limited resources.

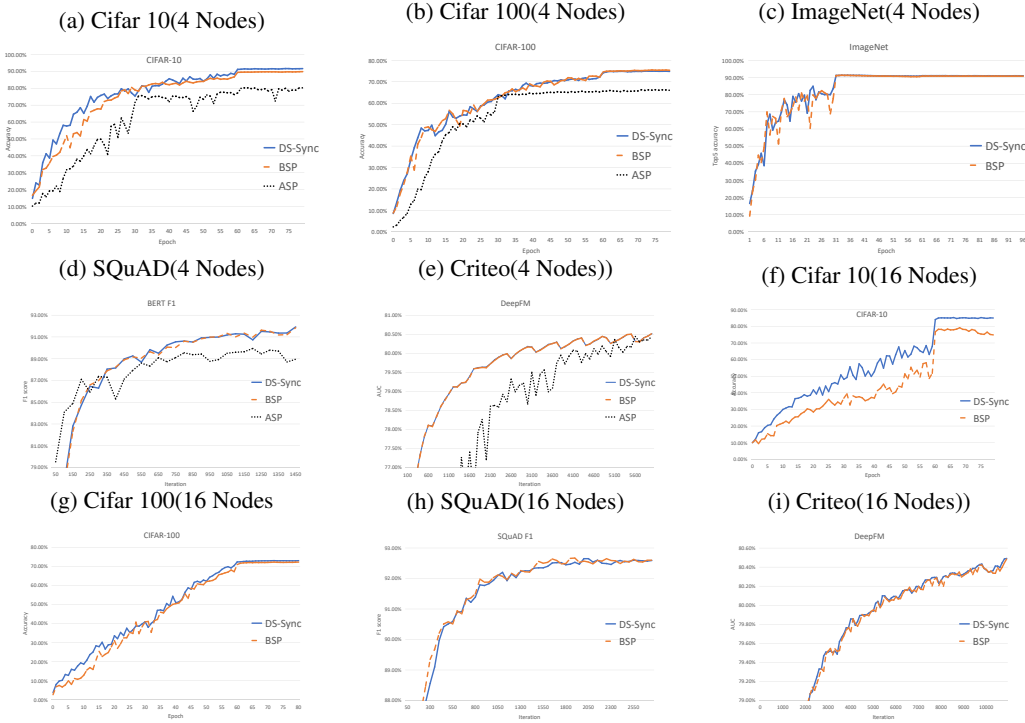


Figure 2: Converging Speed in 4 nodes

4.3 Iteration Overhead Measurement

We quantitatively measure the throughput benefits of DS-Sync on different models by comparing the whole iteration overhead with other baselines. Firstly, we evaluate DS-Sync and all baselines in small-scale scenario of 4 nodes. Since ASP can only use the slow Gloo, we normalize both NCCL and Gloo versions of BSP as the one to fairly compare all methods. From the Figure 3, we can conclude that DS-Sync has advantages over BSP in all models with a speedup of 1.5 times at most. It is even higher than ASP, with only one parameter sever in most cases. The speed up of DS-Sync is positively related to the model parameter size. The smallest model DeepFM with only three FC layers and one embedding layer achieves the lowest speed up because of the limited communication time rate of one iteration.

Further, we also evaluate and compare DS-Sync and BSP in a larger scale scenario of 16 nodes. In the Figure 4, we see considerable more improvements in speed up on all models than the above small scale case. That 16-nodes scenario has a larger synchronization scale indicating more potential room for DS-Sync to improve.

Figure 3: Average iteration overhead measurement in 4 nodes

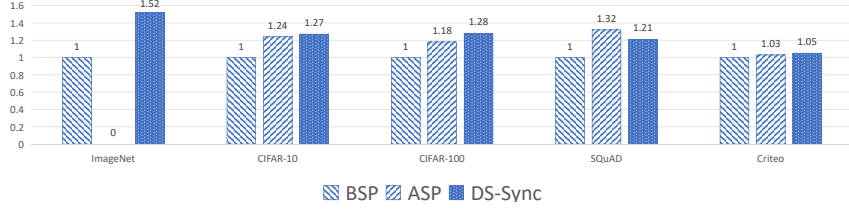
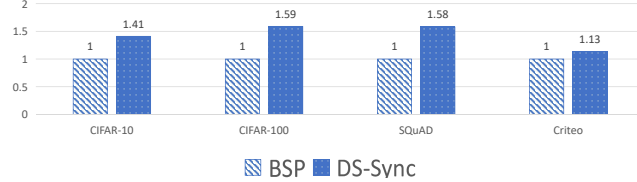


Figure 4: Average iteration overhead measurement in 16 nodes



4.4 Wall-time of Convergence

Finally, we compare DS-Sync with other baselines on the wall time of convergence, which is related to both the iteration number and overhead. We set the mean accuracy minus one std of BSP as the convergence target and record the iteration number and wall time. We omit the results of ASP because it fails to reach the target. Table 4 shows that DS-Sync has significant improvements on the convergence wall time because of both lower iteration overhead and number, especially when overall batch size occupies a large fraction of data set and there are many nodes to form groups. The overall speedup of DS-Sync can surprisingly reach 3.31 times in relatively small data Cifar10 and 16 nodes.

Table 4: Wall-time Analysis

		4 Nodes			16 Nodes		
		Converged Iterations	Wall Time	Speed Up	Converged Iterations	Wall Time	Speed Up
Cifar10	BSP	6566	4011.83	1	1833	1704.69	1
	DS-Sync	2940	1414.14	2.836939766	780	514.8	3.311363636
Cifar100	BSP	12740	7822.36	1	1417	1105.26	1
	DS-Sync	11466	5515.15	1.41834039	806	394.94	2.798551679
ImageNet	BSP	341,664	301,005	1	-	-	-
	DS-Sync	341,664	198,165	1.518961472	-	-	-
SQuAD	BSP	7400	18278	1	2050	7974.5	1
	DS-Sync	7400	15096	1.210784314	1950	4797	1.662393162
Criteo	BSP	5000	20266	1	2260	7137.56	1
	DS-Sync	5000	19300	1.050051813	1980	6676.3	1.069089166

5 Conclusions and Future Works

In this work, we propose DS-Sync that makes contributions in exploring how to reduce the scale of synchronization to speed up. DS-Sync divides workers into multiple parallel groups and at least halves the inevitable serial executed operations. What is more, DS-Sync shuffles the group members every iteration to get global information and maintain the convergence. We also find that Divide-and-Shuffle adds positive side-effects for better generalization. We do quantitative analysis on the scale reduction of DS-sync and interpret its convergence in convex and non-convex cases. The experiments also verify DS-Sync’s significant improvements in the wall-time of converging on realistic scenarios. In future, we plan to extend DS-Sync in the following three directions further:

1. We may investigate DS-Sync in micro scenarios such as synchronization within threads in one GPU or one node. It may inspire new hardware architecture designs such as the new information exchanging mechanism for machine learning.
2. We may explore DS-Sync in macro scenarios such as Federated Learning, where there are thousands of workers and distribution shifting.
3. We may also study different hyperparameters and combine it with other methods and tricks such as gradient compression, local SGD, and warm-up.

References

- [1] Jia Deng, Wei Dong, Richard Socher, Li-Jia Li, Kai Li, and Fei-Fei Li. Imagenet: A large-scale hierarchical image database. In *2009 IEEE Computer Society Conference on Computer Vision and Pattern Recognition (CVPR 2009), 20-25 June 2009, Miami, Florida, USA*, pages 248–255. IEEE Computer Society, 2009.
- [2] Yukun Zhu, Ryan Kiros, Richard S. Zemel, Ruslan Salakhutdinov, Raquel Urtasun, Antonio Torralba, and Sanja Fidler. Aligning books and movies: Towards story-like visual explanations by watching movies and reading books. In *2015 IEEE International Conference on Computer Vision, ICCV 2015, Santiago, Chile, December 7-13, 2015*, pages 19–27. IEEE Computer Society, 2015.
- [3] Sergey Zagoruyko and Nikos Komodakis. Wide residual networks. In Richard C. Wilson, Edwin R. Hancock, and William A. P. Smith, editors, *Proceedings of the British Machine Vision Conference 2016, BMVC 2016, York, UK, September 19-22, 2016*. BMVA Press, 2016.
- [4] Jacob Devlin, Ming-Wei Chang, Kenton Lee, and Kristina Toutanova. BERT: pre-training of deep bidirectional transformers for language understanding. In Jill Burstein, Christy Doran, and Thamar Solorio, editors, *Proceedings of the 2019 Conference of the North American Chapter of the Association for Computational Linguistics: Human Language Technologies, NAACL-HLT 2019, Minneapolis, MN, USA, June 2-7, 2019, Volume 1 (Long and Short Papers)*, pages 4171–4186. Association for Computational Linguistics, 2019.
- [5] Huirong Guo, Ruiming Tang, Yunming Ye, Zhenguo Li, and Xiuqiang He. Deepfm: A factorization-machine based neural network for CTR prediction. In Carles Sierra, editor, *Proceedings of the Twenty-Sixth International Joint Conference on Artificial Intelligence, IJCAI 2017, Melbourne, Australia, August 19-25, 2017*, pages 1725–1731. ijcai.org, 2017.
- [6] Amith R. Mamidala, Jiuxing Liu, and Dhabaleswar K. Panda. Efficient barrier and allreduce on infiniband clusters using multicast and adaptive algorithms. In *2004 IEEE International Conference on Cluster Computing (CLUSTER 2004), September 20-23 2004, San Diego, California, USA*, pages 135–144. IEEE Computer Society, 2004.
- [7] Pitch Patarasuk and Xin Yuan. Bandwidth efficient all-reduce operation on tree topologies. In *21th International Parallel and Distributed Processing Symposium (IPDPS 2007), Proceedings, 26-30 March 2007, Long Beach, California, USA*, pages 1–8. IEEE, 2007.
- [8] Yujun Lin, Song Han, Huizi Mao, Yu Wang, and William J. Dally. Deep gradient compression: Reducing the communication bandwidth for distributed training. *CoRR*, abs/1712.01887, 2017.
- [9] Dan Alistarh, Demjan Grubic, Jerry Li, Ryota Tomioka, and Milan Vojnovic. QSGD: communication-efficient SGD via gradient quantization and encoding. In Isabelle Guyon, Ulrike von Luxburg, Samy Bengio, Hanna M. Wallach, Rob Fergus, S. V. N. Vishwanathan, and Roman Garnett, editors, *Advances in Neural Information Processing Systems 30: Annual Conference on Neural Information Processing Systems 2017, 4-9 December 2017, Long Beach, CA, USA*, pages 1709–1720, 2017.
- [10] Tao Lin, Sebastian U. Stich, Kumar Kshitij Patel, and Martin Jaggi. Don’t use large mini-batches, use local SGD. In *8th International Conference on Learning Representations, ICLR 2020, Addis Ababa, Ethiopia, April 26-30, 2020*. OpenReview.net, 2020.
- [11] Qirong Ho, James Cipar, Henggang Cui, Seunghak Lee, Jin Kyu Kim, Phillip B. Gibbons, Garth A. Gibson, Gregory R. Ganger, and Eric P. Xing. More effective distributed ML via a stale synchronous parallel parameter server. In Christopher J. C. Burges, Léon Bottou, Zoubin Ghahramani, and Kilian Q. Weinberger, editors, *Advances in Neural Information Processing Systems 26: 27th Annual Conference on Neural Information Processing Systems 2013. Proceedings of a meeting held December 5-8, 2013, Lake Tahoe, Nevada, United States*, pages 1223–1231, 2013.
- [12] Eric P. Xing, Qirong Ho, Wei Dai, Jin Kyu Kim, Jinliang Wei, Seunghak Lee, Xun Zheng, Pengtao Xie, Abhimanyu Kumar, and Yaoliang Yu. Petuum: A new platform for distributed machine learning on big data. *IEEE Trans. Big Data*, 1(2):49–67, 2015.
- [13] Amr Ahmed, Mohamed Aly, Joseph Gonzalez, Shravan M. Narayananamurthy, and Alexander J. Smola. Scalable inference in latent variable models. In Eytan Adar, Jaime Teevan, Eugene Agichtein, and Yoelle Maarek, editors, *Proceedings of the Fifth International Conference on*

Web Search and Web Data Mining, WSDM 2012, Seattle, WA, USA, February 8-12, 2012, pages 123–132. ACM, 2012.

- [14] Yucheng Low, Joseph Gonzalez, Aapo Kyrola, Danny Bickson, Carlos Guestrin, and Joseph M. Hellerstein. Distributed graphlab: A framework for machine learning in the cloud. *Proc. VLDB Endow.*, 5(8):716–727, 2012.
- [15] Mu Li, David G. Andersen, Alexander J. Smola, and Kai Yu. Communication efficient distributed machine learning with the parameter server. In Zoubin Ghahramani, Max Welling, Corinna Cortes, Neil D. Lawrence, and Kilian Q. Weinberger, editors, *Advances in Neural Information Processing Systems 27: Annual Conference on Neural Information Processing Systems 2014, December 8-13 2014, Montreal, Quebec, Canada*, pages 19–27, 2014.
- [16] Chia-Yu Chen, Jungwook Choi, Daniel Brand, Ankur Agrawal, Wei Zhang, and Kailash Gopalakrishnan. Adacomp : Adaptive residual gradient compression for data-parallel distributed training. In Sheila A. McIlraith and Kilian Q. Weinberger, editors, *Proceedings of the Thirty-Second AAAI Conference on Artificial Intelligence, (AAAI-18), the 30th innovative Applications of Artificial Intelligence (IAAI-18), and the 8th AAAI Symposium on Educational Advances in Artificial Intelligence (EAAI-18), New Orleans, Louisiana, USA, February 2-7, 2018*, pages 2827–2835. AAAI Press, 2018.
- [17] Alexandros V. Gerbessiotis and Leslie G. Valiant. Direct bulk-synchronous parallel algorithms. *J. Parallel Distributed Comput.*, 22(2):251–267, 1994.
- [18] Benjamin Recht, Christopher Ré, Stephen J. Wright, and Feng Niu. Hogwild: A lock-free approach to parallelizing stochastic gradient descent. In John Shawe-Taylor, Richard S. Zemel, Peter L. Bartlett, Fernando C. N. Pereira, and Kilian Q. Weinberger, editors, *Advances in Neural Information Processing Systems 24: 25th Annual Conference on Neural Information Processing Systems 2011. Proceedings of a meeting held 12-14 December 2011, Granada, Spain*, pages 693–701, 2011.
- [19] Wei Dai, Yi Zhou, Nanqing Dong, Hao Zhang, and Eric P. Xing. Toward understanding the impact of staleness in distributed machine learning. *CoRR*, abs/1810.03264, 2018.
- [20] Sepp Hochreiter and Jürgen Schmidhuber. Flat minima. *Neural Computation*, 9(1):1–42, 1997.
- [21] Alex Krizhevsky, Vinod Nair, and Geoffrey Hinton. The cifar-10 dataset. *online: <http://www.cs.toronto.edu/kriz/cifar.html>*, 55, 2014.
- [22] Pranav Rajpurkar, Jian Zhang, Konstantin Lopyrev, and Percy Liang. Squad: 100, 000+ questions for machine comprehension of text. In Jian Su, Xavier Carreras, and Kevin Duh, editors, *Proceedings of the 2016 Conference on Empirical Methods in Natural Language Processing, EMNLP 2016, Austin, Texas, USA, November 1-4, 2016*, pages 2383–2392. The Association for Computational Linguistics, 2016.
- [23] Xiang Li, Kaixuan Huang, Wenhao Yang, Shusen Wang, and Zhihua Zhang. On the convergence of fedavg on non-iid data. In *8th International Conference on Learning Representations, ICLR 2020, Addis Ababa, Ethiopia, April 26-30, 2020*. OpenReview.net, 2020.

In the appendix, we firstly give the full and formal proof on the convergence of DS-Sync in a simplified scenario. What is more, we also show extra experiments results to compare DS-Sync with the baseline SSP in several datasets.

A DS-Sync Convergence Proof

we give the full and formal convergence proof for DS-Sync in the simplified scenario, namely vanilla SGD optimizer in strongly convex setting. Generally, our proof is very similar with the proofs of FedAvg [23].

A.1 Notation

Firstly, we introduce some changes in the notation for convenience. Let w_t^k be the model parameter in k -th node in the t -th iteration. The update of DS-Sync can be described as

$$v_{t+1}^k = w_t^k - \eta_t \nabla F(w_t^k, \varepsilon_t^k) \quad (3)$$

$$w_{t+1}^k = \frac{1}{N} \sum_{j \in \text{Group}^{(k)}} v_{t+1}^j \quad (4)$$

Here, v_{t+1}^k represents the immediate result of one step SGD update from w_t^k . $F(w_t^k, \varepsilon_t^k)$ is the loss gradient of one local mini-batch ε_t^k . $\text{Group}^{(k)} = \{x|x//N = k//N\}$ if the iteration $(t+1)\%2 = 0$ otherwise $\text{Group}^{(k)} = \{x|x\%N = k\%N\}$. Following previous works, we define two virtual sequences $\bar{v}_t = \frac{1}{N} \sum_{j \in \text{Group}^{(k)}} v_t^j$ and $\bar{w}_t = \frac{1}{N} \sum_{j \in \text{Group}^{(k)}} w_t^j$. Clearly, \bar{v}_{t+1} is the result of one step of SGD from \bar{w}_t . We also define $\bar{g}_t = \frac{1}{N} \sum_{j \in \text{Group}^{(k)}} \nabla F(w_t^k)$ and $g_t = \frac{1}{N} \sum_{j \in \text{Group}^{(k)}} \nabla F(w_t^k, \varepsilon_t^k)$. Hence, we have $\bar{v}_{t+1} = \bar{w}_t - \eta_t g_t$ and $E(g_t) = \bar{g}_t$.

A.2 Assumptions

we formally give all the assumptions in the simplified scenarios as followings:

Assumption A.1. Loss function $F(x)$ is L-smooth for any w and v , namely $F(v) \leq F(w) + (v - w)^T \nabla F(w) + \frac{L}{2} |v - w|^2$

Assumption A.2. Loss function $F(x)$ is μ -strongly convex, namely $F(v) \geq F(w) + (v - w)^T \nabla F(w) + \frac{\mu}{2} |v - w|^2$

Assumption A.3. The variance of stochastic gradients is bounded as $E(|\nabla F(w_t^k, \varepsilon_t^k) - \nabla F(w_t^k)|^2) \leq \sigma^2$

Assumption A.4. The expected squared norm of stochastic gradients is uniformly bounded as $E(|\nabla F(w_t^k, \varepsilon_t^k)|^2) \leq G^2$

A.3 Proofs

We derive the convergence of DS-Sync from 3 key lemmas:

Lemma A.1. (Results of one step vanilla SGD) if $\eta_t \leq \frac{1}{4L}$, we have

$$E(|\bar{v}_{t+1} - w^*|^2) \leq (1 - \eta_t \mu) E(|\bar{w}_t - w^*|^2) + \eta_t^2 E(|g_t - \bar{g}_t|^2) + E\left(\frac{q}{N} \sum_{k \in \text{Group}} |\bar{w}_t - w_t^k|^2\right) \quad (5)$$

Since $\bar{v}_{t+1} = \bar{w}_t - \eta_t g_t$, we have

$$\begin{aligned} |\bar{v}_{t+1} - w^*|^2 &= |\bar{w}_t - \eta_t g_t - w^* - \eta_t \bar{g}_t + \eta_t \bar{g}_t|^2 \\ &= \underbrace{|\bar{w}_t - w^* - \eta_t \bar{g}_t|^2}_{A_1} + \underbrace{2\eta_t \langle \bar{w}_t - w^* - \eta_t \bar{g}_t, \bar{g}_t - g_t \rangle}_{A_2} + \eta_t^2 |\bar{g}_t|^2 \end{aligned} \quad (6)$$

Obviously, the term A_2 has the expectation of 0. Then we focus on the term A_1 and split it into:

$$|\bar{w}_t - w^* - \eta_t \bar{g}_t|^2 = |\bar{w}_t - w^*|^2 - \underbrace{2\eta_t \langle \bar{w}_t - w^*, \bar{g}_t \rangle}_{B_1} + \underbrace{\eta_t^2 |\bar{g}_t|^2}_{B_2} \quad (7)$$

Since $|x|^2$ is a convex function and $F(x)$ is L-smoothness, we have:

$$B_2 = \eta_t^2 |\bar{g}_t|^2 \leq \eta_t^2 \frac{1}{N} \sum_{k \in \text{Group}} |\nabla F(w_t^k)|^2 \leq 2L\eta_t^2 \frac{1}{N} \sum_{k \in \text{Group}} (F(w_t^k) - F^*) \quad (8)$$

For B_1 , we have:

$$\begin{aligned} B_1 &= 2\eta_t \frac{1}{N} \sum_{k \in \text{Group}} \langle \bar{w}_t - w^*, \nabla F(w_t^k) \rangle \\ &= -2\eta_t \frac{1}{N} \sum_{k \in \text{Group}} \langle \bar{w}_t - w_t^k, \nabla F(w_t^k) \rangle - 2\eta_t \frac{1}{N} \sum_{k \in \text{Group}} \langle w_t^k - w^*, \nabla F(w_t^k) \rangle \end{aligned} \quad (9)$$

By Cauchy-Schwarz inequality and AM-GM inequality, we have:

$$-2\eta_t \langle \bar{w}_t - w_t^k, \nabla F(w_t^k) \rangle \leq |\bar{w}_t - w_t^k|^2 + \eta_t^2 |\nabla F(w_t^k)|^2 \quad (10)$$

By the μ -strong convexity of $F(x)$, we have:

$$-2\eta_t \langle w_t^k - w^*, \nabla F(w_t^k) \rangle \leq -2\eta_t (-F(w_t^k) - F(w^*)) - \mu\eta_t |w_t^k - w^*|^2 \quad (11)$$

Then we can bound A_1 by combining equations 8 10 11 and L-smoothness indicates that $\nabla|F(w_t^k)|^2 \leq 2L(F(w_t^k) - F(w^*))$:

$$\begin{aligned} A_1 &= |\bar{w}_t - w^* - \eta_t \bar{g}_t|^2 \leq |\bar{w}_t - w^*|^2 + 2L\eta_t^2 \frac{1}{N} \sum_{k \in \text{Group}} (F(w_t^k) - F(w^*)) \\ &\quad + \frac{1}{N} \sum_{k \in \text{Group}} (|\bar{w}_t - w_t^k|^2 + \eta_t^2 |\nabla F(w_t^k)|^2) \\ &\quad - \frac{1}{N} \sum_{k \in \text{Group}} (2\eta_t (F(w_t^k) - F(w^*)) + \mu\eta_t |w_t^k - w^*|^2) \quad (12) \\ &\leq (1 - \mu\eta_t) |\bar{w}_t - w^*|^2 + \frac{1}{N} \sum_{k \in \text{Group}} |\bar{w}_t - w_t^k|^2 \\ &\quad + \underbrace{\frac{(4L\eta_t^2 - 2\eta_t)}{N} \sum_{k \in \text{Group}} (F(w_t^k) - F(w^*))}_C \end{aligned}$$

To bound C, we have:

$$\begin{aligned} \frac{1}{N} \sum_{k \in \text{Group}} (F(w_t^k) - F(w^*)) &= \frac{1}{N} \sum_{k \in \text{Group}} (F(w_t^k) - F(\bar{w}_t)) + \frac{1}{N} \sum_{k \in \text{Group}} (F(\bar{w}_t) - F(w^*)) \\ &\geq \frac{1}{N} \sum_{k \in \text{Group}} \langle \nabla F(\bar{w}_t), w_t^k - \bar{w}_t \rangle + (F(\bar{w}_t) - F(w^*)) \\ &\geq -\frac{1}{2N} \sum_{k \in \text{Group}} [\eta_t |\nabla F(\bar{w}_t)|^2 + \frac{1}{\eta_t} |w_t^k - \bar{w}_t|^2] + (F(\bar{w}_t) - F(w^*)) \\ &\geq -\frac{1}{N} \sum_{k \in \text{Group}} [\eta_t L(F(\bar{w}_t) - F(w^*)) + \frac{1}{2\eta_t} |w_t^k - \bar{w}_t|^2] + (F(\bar{w}_t) - F(w^*)) \\ &= (1 - \eta_t L)(F(\bar{w}_t) - F(w^*)) - \frac{1}{2N\eta_t} \sum_{k \in \text{Group}} |w_t^k - \bar{w}_t|^2 \quad (13) \end{aligned}$$

where the first inequality is based on the convexity of $F(x)$, the second inequality from AM-GM inequality and the third inequality is according to the L-Smoothness. And we have $F(\bar{w}_t) - F(w^*) \geq 0$. And when $\eta_t < \frac{L}{4}$, it holds that $1 - \eta_t L > \frac{3}{4}$, $(4L\eta_t^2 - 2\eta_t) < 0$ and $(1 - 2L\eta_t) < 1$. It leads to:

$$\begin{aligned} C &= \frac{(4L\eta_t^2 - 2\eta_t)}{N} \sum_{k \in \text{Group}} (F(w_t^k) - F(w^*)) \\ &\leq (4L\eta_t^2 - 2\eta_t)(1 - \eta_t L)(F(\bar{w}_t) - F(w^*)) + \frac{(1 - 2L\eta_t)}{N} \sum_{k \in \text{Group}} |w_t^k - \bar{w}_t|^2 \quad (14) \\ &\leq \frac{1}{N} \sum_{k \in \text{Group}} |w_t^k - \bar{w}_t|^2 \end{aligned}$$

Recalling the expression of A_1 and plugging C into it, we have

$$A_1 = |\bar{w}_t - w^* - \eta_t \bar{g}_t|^2 \leq (1 - \mu\eta_t) |\bar{w}_t - w^*|^2 + 2 \sum_{k \in \text{Group}} |w_t^k - \bar{w}_t|^2 \quad (15)$$

Using the Equatation 14 and taking expecation on both sides of Equation 6, we can complete the proof.

$$E(|\bar{v}_{t+1} - w^*|^2) \leq (1 - \eta_t \mu) E(|\bar{w}_t - w^*|^2) + \eta_t^2 E(|g_t - \bar{g}_t|^2) + E\left(\frac{q}{N} \sum_{k \in \text{Group}} |\bar{w}_t - w_t^k|^2\right) \quad (16)$$

Lemma A.2. (Bounding the variance) Assume Assumption A.3 holds, we have

$$E(|g_t - \bar{g}_t|^2) \leq \frac{\sigma^2}{N} \quad (17)$$

From Assumption A.3, variance of the stochastic gradients in node k is bounded by σ^2 , then

$$\begin{aligned} E(|g_t - \bar{g}_t|^2) &= E\left(\left|\frac{1}{N} \sum_{k \in \text{Group}} [\nabla F(w_t^k, \varepsilon_t^k) - \nabla F(w_t^k)]\right|^2\right) \\ &= \frac{1}{N^2} \sum_{k \in \text{Group}} E(|\nabla F(w_t^k, \varepsilon_t^k) - \nabla F(w_t^k)|^2) \quad (18) \\ &\leq \frac{1}{N^2} \sum_{k \in \text{Group}} \sigma^2 = \frac{\sigma^2}{N} \end{aligned}$$

Lemma A.3. (Bounding the divergence of w_t^k) Assume Assumption A.4 holds, that η_t is non-increasing. It follows that

$$E\left(\frac{1}{N} \sum_{k \in \text{Group}} |\bar{w}_t - w_t^k|^2\right) \leq 4\eta_t^2 G^2 \quad (19)$$

Since DS-Sync forms the same groups every 2 iterations. Namely, the group members in iteration t has met each other in the iteration $t - 2$ and k -th node has met other members in the iteration $t - 1$. For any member j in $group^k$, we have $w_{t-2}^j = \bar{w}_t - 2$. Addtionaly, we have $\eta_{t_2} \leq 2\eta t$ then we have:

$$\begin{aligned} E\left(\frac{1}{N} \sum_{k \in \text{Group}} |\bar{w}_t - w_t^k|^2\right) &= E\frac{1}{N} \sum_{k \in \text{Group}} |(w_t^k - \bar{w}_{t-2}) - (\bar{w}_t - \bar{w}_{t-2})|^2 \\ &\leq E\frac{1}{N} \sum_{k \in \text{Group}} |w_t^k - \bar{w}_{t-2}|^2 \\ &\leq \frac{1}{N} \sum_{k \in \text{Group}} E(\eta_{t-2} |F(w_{t-2}^k, \varepsilon_{t-2}^k)|^2) + E(\eta_{t-1} |F(w_{t-1}^k, \varepsilon_{t-1}^k)|^2) \\ &\leq \frac{1}{N} \sum_{k \in \text{Group}} 2\eta_{t-2}^2 G^2 \leq 4\eta_t^2 G^2 \quad (20) \end{aligned}$$

Theorem A.4. Let Assumptions from A.1 to A.4 hold and L, μ, σ, G be defined. Choose learning rate $\eta_t = \frac{2}{\mu(\gamma+t)}$, then DS-Sync satisfies

$$E[F(\bar{w}_t)] - F(w^*) \leq \frac{2k}{\gamma+t} \left(\frac{B}{\mu} + 2L|w_0 - w^*|^2 \right) \text{quadwhere } B = \frac{\sigma^2}{N} + 8G^2 \quad (21)$$

It is clear that we always have $\bar{w}_{t+1} = \bar{v}_{t+1}$. Let $\Delta_t = E|\bar{w}_t - w^*|^2$. From Lemmas A.1 A.2 A.3, it follows that

$$\Delta_{t+1} \leq (1 - \eta_t \mu) \Delta_t + \eta_t^2 B \quad \text{where } B = \frac{\sigma^2}{N} + 8G^2 \quad (22)$$

For a diminishing learning rate $\eta_t = \frac{\beta}{t+\gamma}$ for some $\beta > \frac{1}{\mu u}$ and $\gamma > 0$, $\eta_1 \leq \min(\frac{1}{u}, \frac{1}{4L}) = \frac{1}{4L}$ and $\eta_t < 2\eta_{t+2}$. We will prove $\Delta_t \leq \frac{v}{t+\gamma}$ where $v = \max(\frac{\beta^2 B}{\beta\mu-1}, (\gamma+1)\Delta_1)$. We use induction to prove it. Firstly, the definition of v ensures that it holds for $t = 1$. Assume the conclusion holds for some t , it follows that

$$\begin{aligned} \Delta_{t+1} &\leq (1 - \eta_t \mu) \Delta_t + \eta_t^2 B \\ &= (1 - \frac{\beta\mu}{t+\gamma}) \frac{v}{t+\gamma} + \frac{\beta^2 B}{(t+\gamma)^2} \\ &= \frac{t+\gamma-1}{(t+\gamma)^2} v + [\frac{\beta^2 B}{(t+\gamma)^2} - \frac{\beta\mu-1}{(t+\gamma)^2} v] \\ &\leq \frac{v}{t+\gamma+1} \end{aligned} \quad (23)$$

Then by the strong convexity $F(x)$,

$$E[F(\bar{w}_t)] - F(w^*) \leq \frac{L}{2} \Delta_t \leq \frac{L}{2} \frac{v}{\gamma+t} \quad (24)$$

If we choose $\beta = \frac{2}{\mu}$, $\gamma = \max(8\frac{L}{\mu}, 2)$ and denote $k = \frac{L}{\mu}$, $\eta_t = \frac{2}{\mu(\gamma+t)}$, we have

$$E[F(\bar{w}_t)] - F(w^*) \leq \frac{2k}{\gamma+t} \left(\frac{B}{\mu} + 2L\Delta_0 \right) \quad (25)$$

B Extra Experiments

Table 5: Converged Accuracy Comparison with SSP in 4 nodes

	Accuracy	LogLoss	Exact Match	F1	AUC	LogLoss
Cifar10	BSP	90.00%($\pm 1.69\%$)	0.4655($\pm 0.0881\%$)	SQuAD	86.85%($\pm 0.53\%$)	93.06%($\pm 0.22\%$)
	ASP	87.46%($\pm 1.31\%$)	0.5348($\pm 0.0676\%$)		82.72%($\pm 0.46\%$)	89.94%($\pm 0.36\%$)
	SSP	89.43%($\pm 2.10\%$)	0.4821($\pm 0.0465\%$)		83.05%($\pm 0.39\%$)	90.15%($\pm 0.45\%$)
	DS-Sync	91.63%($\pm 0.76\%$)	0.4082($\pm 0.0424\%$)		86.83%($\pm 0.56\%$)	93.01%($\pm 0.26\%$)

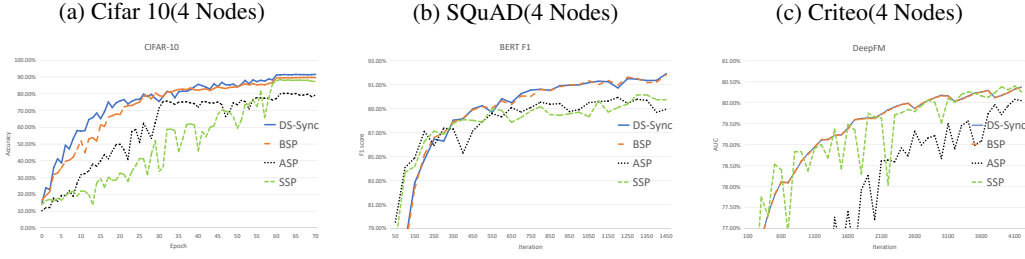


Figure 5: Converging Speed with SSP in 4 nodes

We conduct some extra experiments on SSP to show DS-Sync's advantages on 3 data sets Cifar10, SQuAD, and Criteo and in the small-scale case of 4 nodes. The Table 5 shows that SSP may be better than ASP but still lower than DS-Sync and BSP. And on a larger scale, it is also inclined to fail to

converge properly. We do not extend it to more data sets and scenarios due to limited computing resources and time.

We also compare the converging speed of SSP with DS-Sync. The Figure 5 shows that the learning curve of SSP is not so stable and usually converge to a relatively worse point.